

Influence of a knot on the strength of a polymer strand

A. Marco Saitta*, Paul D. Soper†, E. Wasserman†, and Michael L. Klein*

*Center for Molecular Modeling, Dept. of Chemistry, University of Pennsylvania, Philadelphia, PA 19104-6202, USA

†DuPont Central Research and Development, Expt. Station, Wilmington, DE 19880-0328, USA

(September 7, 2018)

Many experiments have been done to determine the relative strength of different knots, and these show that the break in a knotted rope almost invariably occurs at a point just outside the ‘entrance’ to the knot¹. The influence of knots on the properties of polymers has become of great interest, in part because of their effect on mechanical properties². Knot theory^{3,4} applied to the topology of macromolecules^{5–8} indicates that the simple trefoil or ‘overhand’ knot is likely to be present with high probability in any long polymer strand^{9–12}. Fragments of DNA have been observed to contain such knots in experiments^{13,14} and computer simulations¹⁵. Here we use *ab initio* computational methods¹⁶ to investigate the effect of a trefoil knot on the breaking strength of a polymer strand. We find that the knot weakens the strand significantly, and that, like a knotted rope, it breaks under tension at the entrance to the knot.

Little is known about the structure and properties of knots at the atomic level. For example, the minimum number of carbon atoms that can be sustained as a trefoil in a polyethylene strand is not well established^{5,19}. Polyethylene is the simplest polymer and therefore an excellent generic system to study the fundamental properties of a knotted chain. (Rigorously, a knot is a closed loop; but here, as in ref. 1, we apply the term to a strand with unlinked ends. As a representative polyethylene-like system we chose the linear molecule *n*-decane (C₁₀H₂₂). Empirical models that utilize force constants for bond stretch, bend and torsion^{18–20}, although useful for studying bulk properties of chain molecules, are not applicable to the case of chain rupture. First-principles calculations¹⁶, on the other hand, have been shown to yield satisfactory results for structural and mechanical properties of hydrocarbon-based polymeric systems^{21,22}. The *ab initio* equilibrium structural parameters, after optimization, are in excellent agreement with experiment, with errors in bond lengths and angles smaller than 1% (ref. 22). We studied the response of the *n*-decane molecule to uniaxial strain by systematically increasing the separation *L* between the terminal carbon atoms. For a fixed value of this separation the system was heated to room temperature and then cooled via a simulated annealing technique. The decane molecule remained intact for an elongation up to 18.5% beyond its equilibrium length. Deviations of the C₁-C₂ and C₉-C₁₀

bond lengths from the mean value increase significantly with the applied strain. Under maximum loading the terminal bonds become stretched to $\sim 1.8\text{\AA}$ compared with $\sim 1.7\text{\AA}$ for the others and the terminal C-C-C bond angles increase to ~ 135 deg.

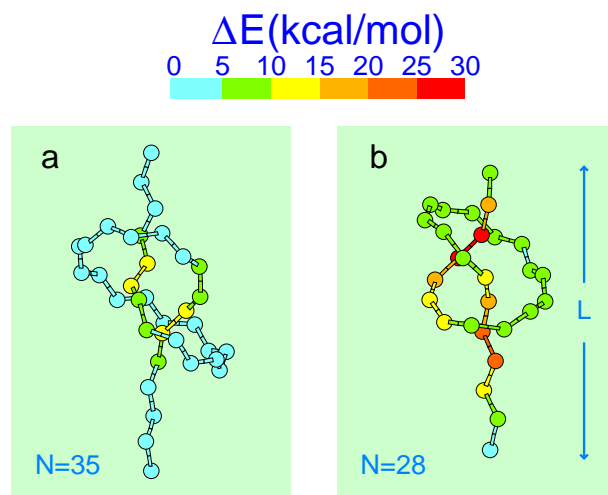


FIG. 1. Strain energy distribution in a knotted polymer strand. Shown are distributions in chains of 35 (a) and 28 (b) carbon atoms taken from constrained classical MD simulations. When the knot is sufficiently tightened, the strain energy localizes mostly on the bonds immediately outside its entrance points.

For larger elongation the molecule dissociates into two radicals with $\text{C}_{10}\text{H}_{22} \rightarrow \text{C}_9\text{H}_{19}\cdot + \text{CH}_3\cdot$. The bond that dissociates involves (randomly) one of the two atoms where the tension is applied. We obtain 83 kcal mol^{-1} for the dissociation energy for the methyl group, which compares favourably with the experimental dissociation enthalpy of $\sim 87 \text{ kcal mol}^{-1}$. A similar calculation performed for *n*-undecane, C₁₁H₂₄, but with the tension still applied to the C₁ and C₁₀ atoms, shows that the C₉-C₁₀ bond breaks to yield an ethyl radical. The calculated dissociation energy in this case is 81 kcal mol^{-1} compared with the experimental enthalpy of $\sim 82 \text{ kcal mol}^{-1}$. As in the previous case, the hybridization of the two key carbon atoms changes from the initial tetrahedral sp^3 to planar sp^2 on formation of the product radicals.

To generate a starting configuration for the *ab initio* study we first performed classical molecular dynamics (MD) calculations on a loosely knotted polyethylene-

like alkane chain, with $N=144$ carbon atoms, in which a trefoil was introduced by adding an appropriate set of *gauche* defects¹⁷. The potential model employed was based on the united atom scheme^{18,19} but with *ab initio* intra-chain stretch and bend force constants taken from the present study. MD calculations were carried out on the knotted chain for a sequence of increasing (constrained) end-to-end distances, L , which gradually resulted in a tighter knot. For any given L , 200 ps of room temperature dynamics, followed by 50 ps of slow cooling, was utilized to relax the system in the trefoil configuration²³. (This run length seemed appropriate given that even the slowest longitudinal phonons can propagate along the entire length of the molecule about 1,000 times during this trajectory.)

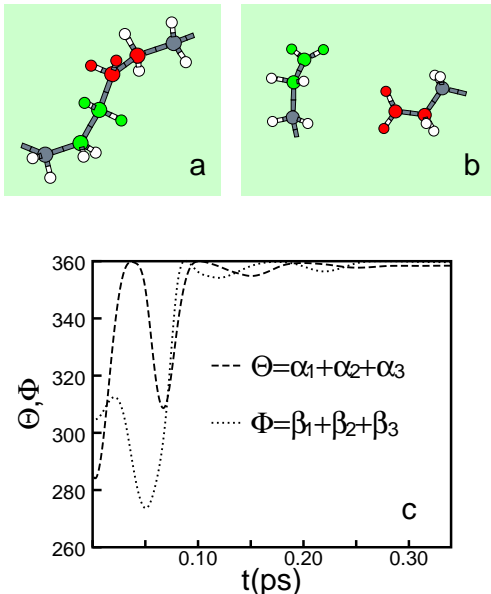


FIG. 2. Analysis of chain rupture. The breakpoint in a $N=28$ trefoil before (a) and after (b) chain dissociation, with C_{22} and C_{23} and their neighbouring atoms highlighted in green and red respectively. Panel c shows the time evolution of the sum of the respective bond angles, which reveals an asymptotic sp^2 hybridization of the carbons involved in the break. The calculations are based on density functional theory with Becke and Lee-Yang-Parr (BLYP)^{24,25} corrections to the exchange and correlation functionals, respectively. Electronic spin polarization has been included within the local spin-density approximation scheme. A valence electron pseudopotential scheme is employed with a plane-wave kinetic-energy cutoff at 60 Ry and a Γ -point sampling of the Brillouin zone. The simulation supercell is large enough to avoid interactions with periodic images.

The global (either constrained or unconstrained) minimum corresponds to an unknotted polymer, but the migration barrier for the knot to propagate along the chain, and thus the disentanglement time, increases dramatically as the trefoil tightens. Thus even at room temperature the system is ‘trapped’ in the knotted configuration

for the timescale of the calculations. Under these circumstances, the portions of the chain far from the trefoil, although extremely important in disentanglement processes, are likely to have little or no effect on the behavior of the knot under stress. Accordingly, as the knot was tightened, atoms far from it were removed from the chain, in order to eventually make the system tractable with first-principles methods.

For each classical MD calculation, we monitored the strain distribution along the chain. Even for $N = 50$, the chain with a trefoil stores a rather small amount of strain energy. However, when the chain was shortened to $N=35$ a pronounced inhomogeneity appeared in the strain energy distribution (Fig. 1a). The shape of the strain energy distribution is essentially the same, at a given L , independent of the details of the simulation, such as the initial configuration and temperature or the length of the MD simulation or a reasonable change in the interaction potentials. (The potentials that we have employed in the MD simulations were all fitted to the properties of alkane molecules close to their equilibrium structures. Thus, in the present case where we are dealing with highly distorted systems, the model’s force constants are likely to yield only semi-quantitative results.) Further shortening of the chain to $N=28$ produced a trefoil (Fig. 1b) with distortions in bond lengths and angles still below the critical values that yield bond breaking in the linear alkanes.

The constrained equilibrium positions obtained from the 250 ps of classical MD evolution of the C_{28} *n*-alkane provided the carbon skeleton of the starting configuration for the first-principles study of the $C_{28}H_{58}$ molecule. A series of Car-Parrinello MD (CPMD) simulations^{16,23–25} were carried out with the separation between C_1 and C_{28} fixed at distances L between 11.50 and 14.00 Å. In each case, the system was allowed to evolve dynamically at room temperature, after which it was cooled. Typically, during the dynamical evolution individual bonds undergo large amplitude thermal fluctuations, which decrease on cooling.

During the room temperature $L = 13.50$ Å CPMD run for $N=28$, dissociation occurred at a bond location, just outside the entrance to the knot, well separated from the terminal atom where the tension was applied. Figure 2 shows the region of the knot where the chain actually ruptured, both before (Fig. 2a) and after (Fig. 2b) the break. The change in hybridization of the C_{22} and C_{23} atoms from sp^3 to sp^2 is clearly evident also in Fig. 2c, where we display the time evolution of the system immediately before and after the break. Figure 3 shows a snapshot of the electronic charge density after the break occurred. The gap in the charge density between the C_{22} and C_{23} atoms confirms the bond breaking at this position. Other simulations carried out with $L \geq 13.50$ Å yield breakpoints at one of the two bonds coming out from the knot²⁵. (Density-functional energy barriers are

not quantitatively very accurate, but the general qualitative description of phenomena, as well as the dissociation energies involved in such processes, are known to be quite reliable.)

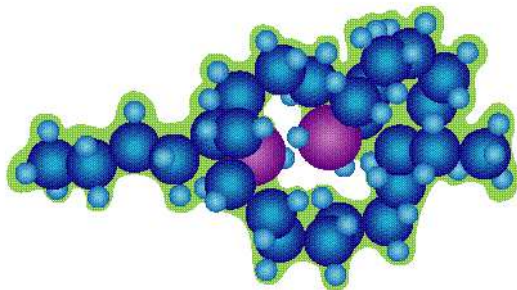


FIG. 3. Schematic electron charge density immediately after the break. Carbon and hydrogen atoms are displayed with spheres corresponding to their respective covalent radii. The green area is a contour plot of the region containing 87% of the total electronic charge. A gap in the charge density, and thus bond-breaking, is observable between the two highlighted C atoms.

The first-principles CPMD calculations provide the total strain energy but not its profile along the chain. The latter can be obtained by making use of an *ab initio* force constants model, which is able to reproduce the total strain energy to $\sim 20\%$. Figure 4 shows the evolution of the strain energy distribution during structural relaxation of a $N=30$ trefoil just before breaking occurs. The strain energy is mainly localized in the two symmetric bonds that are outside the entrance to the knot. Our calculations suggest that 23 carbon atoms form the tightest knot that can be sustained in a polyethylene strand without it breaking.

The strain energy stored in the knot at breaking point is $12.7 \text{ kcal mol}^{-1}$ per C-C bond, which is considerably smaller than the value $16.2 \text{ kcal mol}^{-1}$ for the linear unknotted case. Thus, we find that the presence of the knot has significantly weakened the strand in which it is tied.

While the dynamical evolution of the present constrained *ab initio* MD simulations was sufficient to observe bond breaking, no attempt was made to allow for recombination of the resulting radicals or reactions of the radicals with other parts of the chain. The study of these effects as well as the role of chain branching and the influence of neighbouring chains is left for future research. These factors will likely provide a deeper understanding of how the interplay between inter- and intra-molecular effects contributes to the mechanical properties of real polymer samples².

Note added in proof: Arai *et al.*²⁶ have recently reported the knotting of actin filaments and DNA molecules using optical tweezers. They find that the breaking stress for actin is significantly lower than that of the unknotted filaments, and that the breakage point is at the entrance to the knot, as our calculations predict.

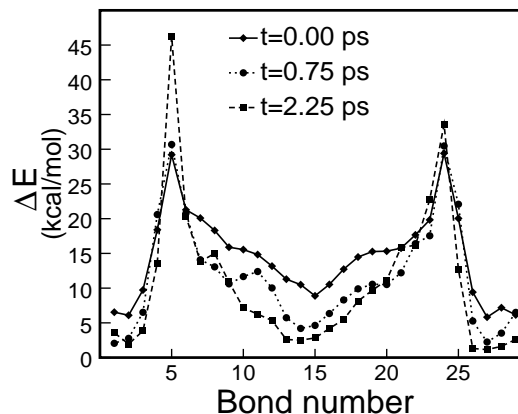


FIG. 4. Relaxation of the strain energy distribution. Shown is the distribution along a $C_{30}H_{62}$ chain containing a trefoil during CPMD energy minimization at $T = 0K$. The $t = 0$ configuration is an average of the equilibrium positions obtained along classical MD simulations performed with different initial states and temperatures. The segments outside the knot and its central portion relax, while stress tends to concentrate mostly on the two entrance bonds (see Fig.1).

1. Ashley, C.W. The Ashley Book of Knots (Doubleday, New York, 1993).
2. Bayer, R.K. Structure transfer from a polymeric melt to the solid state Part III: Influence of knots on structure and mechanical properties of semicrystalline polymers. *Colloid Polym. Sci.* **272**, 910-932 (1994).
3. Atiyah, M.F. The geometry and physics of knots (Cambridge University Press, 1990).
4. Katritch., V. *et al.* Geometry and physics of knots. *Nature* **384**, 142-145 (1996); Katritch., V. *et al.* Properties of ideal composite knots. *Nature* **388**, 148-151 (1997).
5. Frisch, H.L. & Wasserman, E. Chemical topology. *J. Am. Chem. Soc.* **83**, 3789-3795 (1961).
6. Mislow, K. Introduction to stereochemistry (W.A. Benjamin, New York, 1965).
7. Schill, G. Catenanes, Rotaxanes, and Knots (Academic, New York, 1971).
8. Walba, D.M. Topological stereochemistry. *Tetrahedron* **41**, 3161-3212 (1985).
9. Frank-Kamenetskii, M.D., Lukashin, A.V. & Vologodskii, A.V. Statistical mechanics and topology of polymer chains. *Nature* **258**, 398-402 (1975).
10. Frisch, H.L. Macromolecular topology - Metastable isomers from pseudo interpenetrating polymer network. *New J. Chem.* **17**, 697-701 (1993).
11. Mansfield, M.L. Knots in hamiltonian cycles. *Macromolecules* **27**, 5924-5926 (1994).
12. van Rensburg, E.J., Sumners, D.A.W., Wasserman, E. & Whittington, S.G. Entanglement complexity of self-avoiding walks. *J. Phys. A.* **25**, 6557-6566 (1992).
13. Wasserman, S.A. & Cozzarelli, N.R. Biochemical topology: applications to DNA recombination and replication. *Science* **232**, 951-960 (1986).
14. Shaw, S.Y. & Wang, J.C. Knotting of a DNA chain during ring closure. *Science* **260**, 533-536 (1993).
15. Schlick, T. & Olson, W.K. Trefoil knotting revealed by molecular dynamics simulations of supercoiled DNA. *Science* **257**, 1110-1115 (1992).

16. Car, R. & Parrinello, M. Unified approach for molecular dynamics and density-functional theory. *Phys. Rev. Lett.* **55**, 2471-2474 (1985).
17. de Gennes, P.-G. Tight knots. *Macromolecules* **17**, 703-704 (1984).
18. Siepmann, J.I., Karaborni, S. & Smit, B. Simulating the critical-behavior of complex fluids. *Nature* **365**, 330-332 (1993).
19. Mundy, C.J., Balasubramanian, S., Bagchi, K., Siepmann, J.I. & Klein, M.L. Equilibrium and non-equilibrium simulation studies of fluid alkanes in bulk and at interfaces. *Faraday Discuss.* **104**, 17-36 (1996).
20. Karasawa, N., Dasgupta, S. & Goddard, W.A. III Mechanical properties and force-field parameters for polyethylene crystal. *J. Phys. Chem. US* **95**, 2260-2272 (1991).
21. Ancilotto, F., Chiarotti, G.L., Scandolo S. & Tosatti E. Dissociation of methane into hydrocarbons at extreme (planetary) pressure and temperature. *Science* **275**, 1288-1290 (1997).
22. Montanari, B. & Jones, R.O. Density functional study of crystalline polyethylene. *Chem. Phys. Lett.* **272**, 347-352 (1997), and references therein.
23. Martyna, G.J. et al. PINY Code. *Comp. Phys. Comm.* (in the press).
24. Becke, A.D. Density-functional exchange-energy approximation with correct asymptotic behavior. *Phys. Rev. A* **38**, 3098-3100 (1988)
25. Lee, C., Yang, W. & Parr, R.G. Development of the Colle-Salvetti correlation-energy formula into a functional of the electron density. *Phys. Rev. B* **37**, 785-789 (1988).
26. Arai, T. *et al.* Tying a molecular knot with optical tweezers. *Nature* (in the press).

Acknowledgements. The work was supported in part by the National Science Foundation.

Correspondence and request for material should be addressed to M.L.K. (e-mail: klein@lrsm.upenn.edu).
